# Physical forcing and the dynamics of the pelagic ecosystem in the eastern tropical Pacific: simulations with ENSO-scale and global-warming climate drivers

**George M. Watters, Robert J. Olson, Robert C. Francis, Paul C. Fiedler, Jeffrey J. Polovina, Stephen B. Reilly, Kerim Y. Aydin, Christofer H. Boggs, Timothy E. Essington, Carl J. Walters, and James F. Kitchell**

**Abstract:** We used a model of the pelagic ecosystem in the eastern tropical Pacific Ocean to explore how climate variation at El Niño – Southern Oscillation (ENSO) scales might affect animals at middle and upper trophic levels. We developed two physical-forcing scenarios: (1) physical effects on phytoplankton biomass and (2) simultaneous physical effects on phytoplankton biomass and predator recruitment. We simulated the effects of climate-anomaly pulses, climate cycles, and global warming. Pulses caused oscillations to propagate through the ecosystem; cycles affected the shapes of these oscillations; and warming caused trends. We concluded that biomass trajectories of single populations at middle and upper trophic levels cannot be used to detect bottom-up effects, that direct physical effects on predator recruitment can be the dominant source of interannual variability in pelagic ecosystems, that such direct effects may dampen top-down control by fisheries, and that predictions about the effects of climate change may be misleading if fishing mortality is not considered. Predictions from ecosystem models are sensitive to the relative strengths of indirect and direct physical effects on middle and upper trophic levels.

**Résumé :** Un modèle de l'écosystème pélagique du Pacifique oriental tropical nous a permis d'explorer comment des variations à l'échelle d'El Niño et de l'oscillation australe (ENSO) peuvent affecter les animaux des niveaux trophiques moyens et supérieurs. Nous avons imaginé deux scénarios de forçage physique : (1) les effets physiques sur la biomasse du phytoplancton et (2) les effets physiques simultanés sur la biomasse du phytoplancton et le recrutement des prédateurs. Nous avons simulé les effets des pulsations des anomalies climatique, de cycles climatiques et du réchauffement global. Les pulsations engendrent des oscillations qui se propagent dans l'écosystème, les cycles modifient la forme des oscillations et le réchauffement global engendre des tendances. Nos conclusions sont les suivantes : les trajectoires de la biomasse de populations isolées des niveaux trophiques moyens ou supérieurs ne peuvent servir à déceler les effets ascendants; les effets physiques qui affectent directement le recrutement des prédateurs peuvent être la source principale de la variation inter-annuelle dans les écosystèmes pélagiques; de tels effets directs peuvent tamponner le contrôle descendant exercé par la pêche commerciale; les prédictions sur les effets des changements climatiques peuvent être trompeurs, si on ne tient pas compte de la mortalité des poissons due à la pêche. Les prédictions des

Received 2 August 2002. Accepted 19 July 2003. Published on the NRC Research Press Web site at http://cjfas.nrc.ca on 21 October 2003.
J17023

**G.M. Watters[1,2] and R.J. Olson.** Inter-American Tropical Tuna Commission, 8604 La Jolla Shores Drive, La Jolla, CA 92037, U.S.A.
**R.C. Francis.** School of Aquatic and Fisheries Sciences, University of Washington, Box 355020, Seattle, WA 98195, U.S.A.
**P.C. Fiedler and S.B. Reilly.** NOAA Fisheries, Southwest Fisheries Science Center, P.O. Box 271, La Jolla, CA 92038, U.S.A.
**J.J. Polovina and C.H. Boggs.** NOAA Fisheries, Honolulu Laboratory, 2570 Dole Street, Honolulu, HI 96822, U.S.A.
**K.Y. Aydin.** School of Aquatic and Fisheries Sciences, University of Washington, Box 355020, Seattle, WA 98195, U.S.A., and NOAA Fisheries, Alaska Fisheries Science Center, 7600 Sandpoint Way NE, Seattle, WA 98115, U.S.A.
**T.E. Essington.** NOAA Fisheries, Honolulu Laboratory, 2570 Dole Street, Honolulu, HI 96822, U.S.A., Center for Limnology, University of Wisconsin, 680 North Park Street, Madison, WI 53706, U.S.A., and Marine Sciences Research Center, Stony Brook University, Stony Brook, NY 11794, U.S.A.
**C.J. Walters.** Fisheries Centre, University of British Columbia, 6660 NW Marine Drive, Building 022, Vancouver, BC 6VT 124, Canada.
**J.F. Kitchell.** Center for Limnology, University of Wisconsin, 680 North Park Street, Madison, WI 53706, U.S.A.

[1]Corresponding author (e-mail: George.Watters@noaa.gov).
[2]Present address: NOAA Fisheries, Pacific Fisheries Environmental Laboratory, 1352 Lighthouse Avenue, Pacific Grove, CA 93950, U.S.A.

 doi: 10.1139/F03-100 

modèles d'écosystèmes sont aussi affectées par l'importance relative des effets physiques directs et indirects sur les niveaux trophiques moyens et supérieurs.

[Traduit par la Rédaction]

## Introduction

The ability of physical processes to structure ecosystems must be considered when measuring the top-down effects of fishing. We used a food-web model to explore how climate might affect the pelagic ecosystem in the eastern tropical Pacific Ocean (ETP). Previous workers have studied predator–prey interactions in the ETP (e.g., Olson and Boggs 1986; Robertson and Chivers 1997), but how these interactions structure the pelagic food web during climate variation has not been described.

Plant and animal populations in the ETP are affected by the El Niño – Southern Oscillation (ENSO). Several workers have documented a connection between the ENSO and both the rate of primary production and phytoplankton biomass in the ETP. The production rate is generally decreased during warm El Niño periods and increased during cold La Niña periods (e.g., Barber and Chavez 1983; Fiedler et al. 1992; Barber et al. 1996). Phytoplankton biomass can also be reduced during El Niños and increased during La Niñas (e.g., Fiedler et al. 1992; Barber et al. 1996; Bidigare and Ondrusek 1996). In addition to affecting plant productivity and biomass, the ENSO affects the species composition of the phytoplankton. In general, the ENSO affects the biomass of large (>5 μm) phytoplankton more than that of small (≤5 μm) phytoplankton (e.g., Bidigare and Ondrusek 1996; Landry et al. 1996). The ENSO also affects animals at middle and upper trophic levels. For example, Barber and Chavez (1983) concluded that the 1982–1983 El Niño reduced the growth rates and reproductive successes of various birds, mammals, and fishes.

Several coupled ocean-atmosphere models describe how the ENSO might respond to increased atmospheric concentrations of greenhouse gases during the 21st century. These models generally predict that mean sea-surface temperatures (SSTs) in the tropical Pacific Ocean will increase, but they do not agree on the future frequency and amplitude of ENSO cycling in the ETP. Timmermann et al. (1999) and Collins (2000*a*) predict an increase in both the amplitude and frequency of the ENSO, but Collins et al. (2001) do not predict significant changes in these statistics. Alternative hypotheses about the consequences of greenhouse warming for SSTs may lead to different predictions about the future structure of the pelagic ecosystem.

Our work has three objectives. The first is to explore how a single, ENSO-scale climate pulse might affect the middle and upper trophic levels of the pelagic ecosystem in the ETP. Second, we explore how the ecosystem might respond to changes in the periodicity of warm and cold events during sustained ENSO-scale cycling. Finally, we explore how greenhouse warming might affect the pelagic ecosystem in the ETP. We address these three objectives by simulating physical forcing events in a food-web model developed by Olson and Watters (2003). Although the focus of our work is on the ETP, we believe that many of our results can be generalized to other pelagic marine ecosystems.

## Methods

### System and model descriptions

We used a model developed and documented by Olson and Watters (2003). This model was assembled in Ecopath with Ecosim (EwE) (Walters et al. 2000) and contains 38 components (Table 1). Some components are split into two biomass pools based on length (Table 1). We identify the large and small fishes from these split pools with the respective abbreviations "Lg" and "Sm". Substantial uncertainty surrounds many of the parameters in Table 1. The model focuses on pelagic regions of the ETP, and coastal ecosystems are not adequately described.

Temporal dynamics in Ecosim are largely controlled by food consumption. Walters et al. (2000) provide the equations used in Ecosim, but we condense and reparameterize some of them here. Consumption ($C_{ijt}$) of prey $i$ by predator $j$ at time $t$ depends on the biomasses of both the prey ($B_{it}$) and predator ($B_{jt}$) and can be influenced by environmental conditions:

$$(1) \qquad C_{ijt} = \frac{a_{ij} v_{ij} v^*_{ijt} B_{it} B_{jt}}{2v_{ij} v^*_{ijt} + a_{ij} B_{jt}}$$

where $a_{ij}$ is the effective rate at which predator $j$ searches for prey $i$ and $v_{ij}$ is the maximum instantaneous rate of mortality that predator $j$ can impose on prey $i$; $v^*_{ijt}$ can vary with environmental conditions and is an anomaly in $v_{ij}$ at time $t$. The product of $v_{ij}$ and $v^*_{ijt}$ describes the vulnerability of prey $i$ to predation by predator $j$ at time $t$.

The recruitment ($R_{it}$) of components split into pools of large and small animals can also be affected by environmental conditions (again, Walters et al. (2000) provide detail about the recruitment function).

$$(2) \quad R_{i\,t+1} = f\left( R_{i\,t=0}, \frac{N^{\mathrm{Lg}}_{it}}{N^{\mathrm{Lg}}_{i\,t=0}}, \frac{\sum_j C^{\mathrm{Lg}}_{jit}}{B^{\mathrm{Lg}}_{it}}, p_{it}, \frac{\sum_j C^{\mathrm{Lg}}_{ji\,t=0}}{B^{\mathrm{Lg}}_{i\,t=0}}, q_{i\,t=0} \right) r^*_{it}$$

Time zero ($t = 0$) refers to the initial conditions described by the parameters in Table 1. $R_{i\,t=0}$ is a baseline recruitment estimated from these parameters. $N^{\mathrm{Lg}}_{it}$ is the simulated abundance of large fish in component $i$ at time $t$, and $B^{\mathrm{Lg}}_{it}$ is their biomass. $p_{it}$ is the time-specific proportion of energy that large fish allocate to reproduction, and $q_{i\,t=0}$ is the proportion of energy that large fish allocate to growth under the initial conditions (note that $q_{i\,t=0} \neq 1 - p_{it}$). $r^*_{it}$ is a time-specific anomaly in the production of eggs (or larvae) that is independent of the biomass of large fish from component $i$ and may be controlled by environmental conditions.

**Table 1.** Parameters for the Ecopath model of the pelagic ecosystem in the eastern tropical Pacific (ETP) (Olson and Watters 2003).

| Component (code for DP) | FL | TL | *B* | *Z* | *Q*/*B* | EE | DP | LD |
|---|---|---|---|---|---|---|---|---|
| Lg marlins[b] | ≥150 | 5.3 | **573** | 1.00 | 7.80 | 0.50 | SYFT (0.25) | × |
| Toothed whales[b] | | 5.2 | 31 000 | 0.02 | 6.75 | **0.00** | CEPH (0.65) | × |
| Lg bigeye[a] | ≥80 | 5.2 | 9 000 | 0.76 | 13.03 | **0.33** | CEPH (0.71) | × |
| Sm marlins[b] | <150 | 5.2 | **145** | 0.50 | 9.00 | 0.75 | *Auxis* (0.20) | × |
| Sm sharks[b] | <150 | 5.2 | **270** | 0.58 | 9.16 | **0.58** | SYFT (0.40) | × |
| Spotted dolphins[a] | | 5.0 | 3 500 | 0.04 | 16.50 | **0.22** | CEPH (0.60) | × |
| Lg swordfish[a] | ≥150 | 5.0 | **33** | 0.44 | 7.80 | 0.75 | CEPH (0.60) | × |
| Lg sailfish[a] | ≥150 | 4.9 | **52** | 1.15 | 7.80 | 0.25 | MMF (0.37) | × |
| Lg wahoo[a] | ≥90 | 4.9 | 1 100 | 1.20 | 9.76 | **0.07** | *Auxis* (0.23) | × |
| Lg sharks[b] | ≥150 | 4.9 | 400 | 0.32 | 7.81 | **0.48** | MEF (0.39) | × |
| Pursuit birds[a] | | 4.8 | 600 | 0.08 | 65.70 | **0.23** | FLY (0.55) | |
| Lg yellowfin[a] | ≥90 | 4.7 | 6 500 | 2.35 | 15.60 | **0.36** | *Auxis* (0.54) | × |
| Sm dorado[a] | <90 | 4.7 | 2 000 | 3.15 | 27.40 | **0.99** | FLY (0.44) | × |
| Mesopelagic dolphins[a] | | 4.6 | 17 000 | 0.04 | 16.50 | **0.19** | MMF (0.54) | × |
| Lg dorado[a] | ≥90 | 4.6 | **218** | 1.20 | 21.90 | 0.25 | FLY (0.55) | × |
| Skipjack[b] | | 4.6 | **26 443** | 1.88 | 21.50 | 0.40 | MEF (0.31) | × |
| Albacore | | 4.6 | **3 026** | 0.77 | 16.95 | 0.75 | MEF (0.54) | × |
| Sm yellowfin[a] (SYFT) | <90 | 4.6 | 8 200 | 1.75 | 18.30 | **0.92** | MEF (0.37) | × |
| Sm sailfish[a] | <150 | 4.6 | **127** | 0.57 | 9.76 | 0.75 | MMF (0.42) | × |
| Sm wahoo[a] | <90 | 4.6 | **2 730** | 1.75 | 11.40 | 0.75 | MEF (0.48) | × |
| Sm bigeye[a] | <80 | 4.5 | 10 000 | 0.72 | 15.25 | **0.69** | MMF (0.58) | × |
| Bluefin[a] | | 4.4 | 1 400 | 0.65 | 12.80 | **0.80** | MEF (0.20) | × |
| Sm swordfish[a] | <150 | 4.4 | **98** | 0.21 | 9.00 | 0.75 | MEF (0.66) | × |
| Cephalopods[c] (CEPH) | | 4.4 | **1 104 807** | 2.00 | 7.00 | 0.85 | MMF (0.42) | |
| Misc. piscivores[a] | | 4.3 | **16 536** | 2.25 | 7.73 | 0.95 | MEF (0.43) | × |
| *Auxis*[c] | | 3.9 | **143 247** | 2.50 | 25.00 | 0.95 | MESZ (0.48) | × |
| Grazing birds[a] | | 3.8 | 123 | 0.15 | 65.70 | **0.13** | MESZ (0.39) | |
| Baleen whales[a] | | 3.8 | 9 100 | 0.02 | 9.10 | **0.00** | MESZ (0.84) | |
| Rays[a] | | 3.7 | 230 | 0.25 | 3.91 | **0.36** | MESZ (0.45) | × |
| Sea turtles[a] | | 3.6 | **260** | 0.15 | 3.50 | 0.50 | MESZ (0.47) | × |
| Crabs[a] | | 3.5 | **119 694** | 3.50 | 10.00 | 0.95 | MESZ (0.46) | |
| Flyingfishes[a] (FLY) | | 3.4 | **160 604** | 2.88 | 25.78 | 0.95 | MESZ (0.60) | |
| Misc. mesopelagic fishes[a] (MMF) | | 3.4 | 2 000 000 | 2.00 | 10.78 | **0.95** | MESZ (0.64) | |
| Misc. epipelagic fishes[b] (MEF) | | 3.2 | **2 248 549** | 2.07 | 10.78 | 0.95 | MESZ (0.48) | × |
| Mesozooplankton (MESZ) | | 2.7 | **706 709** | 64.00 | 200.00 | 0.68 | MICZ (0.70) | |
| Microzooplankton (MICZ) | | 2.0 | **826 425** | 143.00 | 600.00 | 0.98 | SP (1.00) | |
| Lg phytoplankton | | 1.0 | **426 093** | 125.00 | | 0.90 | | |
| Sm producers (SP) | | 1.0 | **2 999 183** | 167.00 | | 0.99 | | |

**Note:** Some parameters are not provided because of space limitations, but the full set can be obtained from the authors. FL, fork length (cm); TL, trophic level; *B*, biomass (t·million km$^{-2}$); *Z*, total mortality rate; *Q*/*B*, consumption to biomass ratio; EE, ecotrophic efficiency; DP, dominant prey in the ETP (proportion of diet); LD, landed or discarded by fisheries in the ETP; Lg, large; Sm, small; Misc., miscellaneous. Values in bold type were estimated by solving the Ecopath mass-balance equations.

[a]The mass-balance solution is relatively insensitive to variation in the parameters for these components (Olson and Watters 2003).

[b]The mass-balance solution is moderately sensitive to variation in the parameters for these components (Olson and Watters 2003).

[c]The mass-balance solution is highly sensitive to variation in the parameters for these components (Olson and Watters 2003).

## Physical forcing of phytoplankton biomass

We used variations in the biomass of large phytoplankton to drive our ecosystem model from the bottom up. We assumed that the ENSO causes variability in the biomass of large phytoplankton, but not in the biomass of small producers. This assumption is consistent with observations that the biomass of diatoms varied substantially during recent warm and cold events, whereas the biomass of picoplankton was relatively stable (Bidigare and Ondrusek 1996; Landry et al. 1996). The effect of assuming that the biomass of small producers did not vary with the ENSO was to decrease the amplitude of bottom-up effects in our simulations.

We created time series of $B_{\text{Lg phytoplankton } t}$ with an empirical model that relates the SST anomolies of the NIÑO3 region (5°N–5°S, 150–90°W) to surface chlorophyll concentrations. During recent warm and cold events, log(pigment concentrations (mg·m$^{-3}$)) in the NIÑO3 region changed by about –0.109/°C (the mean of the rightmost column of values in Table 2). We used this estimate to create time series of large phytoplankton biomass that were representative of ENSO-scale forcing.

$$B_{\text{Lg phytoplankton } t} = B_{\text{Lg phytoplankton } t=0} \cdot \exp(-0.109X_t) \quad (3)$$

**Table 2.** Phytoplankton-pigment data and NIÑO3 sea-surface temperature (SST) anomalies used to construct eq. 3.

| Source of chlorophyll data | Time periods | Mean pigment concentration ($mg \cdot m^{-3}$) in model arena ($P$) | Mean NIÑO3 SST anomaly (°C) ($T$) | Change in log(pigment concentration) per °C $(\ln(P_2/P_1)/(T_2 - T_1))$ |
|---|---|---|---|---|
| Shipboard observations (Fiedler et al. 1992) | (1) Aug.–Nov. 1987 | $P_1 = 0.130$ | $T_1 = +1.71$ | –0.169 |
| | (2) Aug.–Nov. 1988 | $P_2 = 0.222$ | $T_2 = –1.45$ | |
| Monthly coastal zone color scanner data (Tran et al. 1993) | (1) Jan.–April 1983 | $P_1 = 0.081$ | $T_1 = +2.65$ | –0.100 |
| | (2) Jan.–April 1984 | $P_2 = 0.106$ | $T_2 = –0.05$ | |
| Monthly SeaWiFS data (http://seawifs.gsfc.nasa.gov/SEAWIFS.html) | (1) Nov. 1997 – May 1998 | $P_1 = 0.124$ | $T_1 = +2.79$ | –0.058 |
| | (2) Nov. 1998 – May 1999 | $P_2 = 0.151$ | $T_2 = –0.61$ | |

**Note:** The SST anomalies were obtained from the United States National Oceanic and Atmospheric Administration, National Weather Service, Climate Prediction Center, and cover the NIÑO3 area (5°N–5°S, 150–90°W).

$B_{\text{Lg phytoplankton } t=0}$ is the biomass of large phytoplankton from Table 1, and $X_t$ is a NIÑO3 SST anomaly at time $t$. To generate biomass trajectories for large phytoplankton, we entered various time series of SST anomalies (see Simulations) into eq. 3. We used these biomass trajectories to drive the ecosystem model by appropriate substitution of $B_{\text{Lg phytoplankton } t}$ for $B_{it}$ in eq. 1. Thus, we forced the biomass of large phytoplankton to decrease during warm events and increase during cold events. Equation 3 is not suitable for coastal regions of the ETP.

**Physical forcing of predator recruitment**

Forcing our model via eq. 3 can cause predator biomasses to decrease after a warm event, but estimates from Maunder and Watters (2002) suggest that annual recruitments of yellowfin tuna were highest following the 1987 and 1998 El Niños. We addressed this inconsistency with two other empirical models. These two models relate predator recruitment to NIÑO3 SST anomalies and force recruitment to increase during warm events. We forced recruitment to all of the split-pool components except sharks. Shark recruitment was not forced because the shark species represented by our model are viviparous or ovoviviparous. We assumed that environmental effects on recruitment to populations with reproductive modes involving parental care are different from those on oviparous fishes. The effect of this assumption was that sharks did not benefit from warm events as much as other predators.

We hypothesized that environmental conditions might affect the recruitment of predators in split pools by influencing both survival of small fishes and egg production by large fishes. The former type of forcing is consistent with an untested hypothesis that increased growth rates during warm events cause small predators to spend less time inside a window of increased vulnerability to predation. Physical forcing of egg production is consistent with observed relationships between spawning activity by yellowfin (*Thunnus albacares*) and skipjack (*Katsuwonus pelamis*) tunas and SST (Schaefer 1998, 2001).

To specify temporal trends in vulnerability to predation, we first obtained a single estimate of $v_{ij}$ for all predator–prey links in our model (i.e., we assumed that $v_{ij} = v \; \forall \; i$ and $j$). We estimated this parameter by fitting to 28 time series of relative abundance and four time series of total mortality ($Z$) estimates. Some of the abundance indices were generated from the output of single-species stock assessments (large and small yellowfin, large and small bigeye, large and small marlins, albacore, and skipjack) and others were derived from catch-per-unit-effort (CPUE) data (large and small marlins, large and small sharks, large and small sailfish, large swordfish, small dorado, small wahoo, miscellaneous piscivores, rays, sea turtles, and miscellaneous epipelagic fishes). The time series of $Z$s were obtained from single-species stock assessments (large and small yellowfin and bigeye). We estimated that predators could increase the instantaneous rate of predation mortality on their prey to about 1.8 times the rates implied by the parameters in Table 1. With this estimate, our model provided relatively good fits to the stock-assessment data and relatively poor fits to the CPUE data. We were not disappointed by the lack of fit to the CPUE series because it was not likely that variations in the CPUE data reflected actual

**Fig. 1.** Schematic representations of (*a*) the axis of the *Auxis* and (*b*) the axis of the squid. These two axes were defined for the purpose of summarizing our results. Thin arrows indicate that <1% of the total biomass flowing within an axis is being transferred between two components. Arrows of medium thickness indicate that 1–25% of the total biomass flowing within an axis is being transferred, and thick arrows indicate that >25% of the total flow is occurring between two components. Rank production was calculated for all of the components in the ecosystem model (Table 1). Lg, large; Sm, small; Misc., miscellaneous.

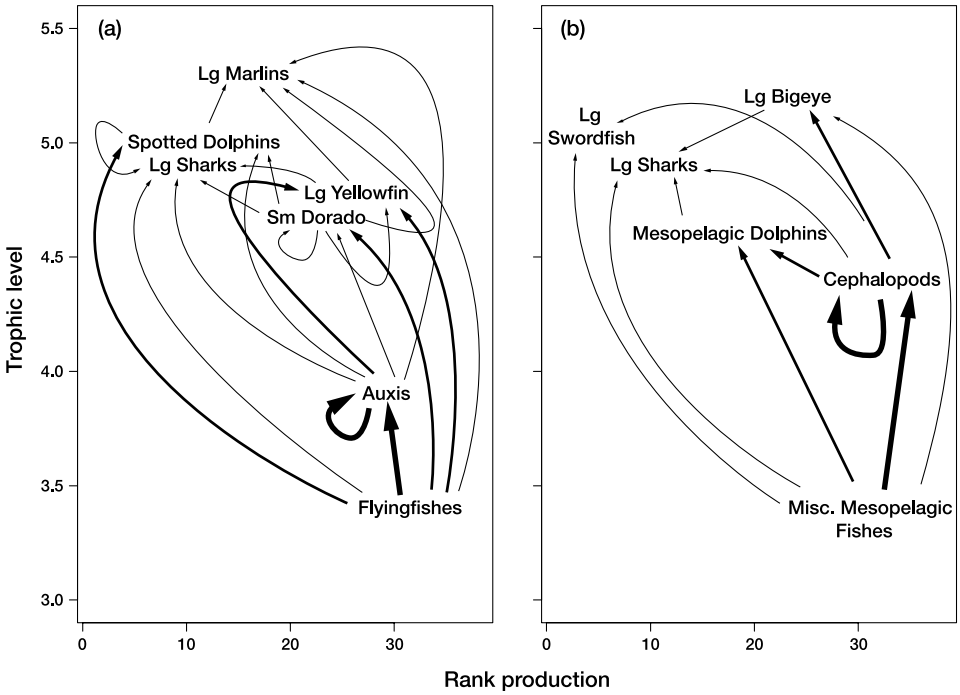


variations in biomass. Rather, these variations were probably the result of changes in catchability and availability. We also note that Olson and Watters (2003) estimated $v_{ij}$ by fitting only to the stock-assessment data for yellowfin and bigeye tunas. Their estimate was similar to ours, and this similarity implies that the CPUE data used here contained relatively little information about vulnerability.

We also generated series of $v^*_{ijt}$ to force temporal trends in predator vulnerability. We used estimates of recruits per spawner from a recent stock assessment of yellowfin tuna (Maunder and Watters 2002) to obtain (via maximum likelihood) the rate parameter of an empirical model describing how vulnerability to predation might vary with changes in SST.

$$(4) \qquad v^*_{ijt} = \exp(-1.271X_t)$$

where $i \in$ {Sm marlins, Sm dorado, Sm yellowfin, Sm sailfish, Sm wahoo, Sm bigeye, Sm swordfish}. We generated series of $v^*_{ijt}$ by entering NIÑO3 SST anomalies (see Simulations) into eq. 4, and we used these series of $v^*_{ijt}$ to drive the ecosystem model by appropriate substitution into eq. 1. Thus, we forced small predators from split-pool components to be less vulnerable to predation during warm events and more vulnerable during cold events.

We also used the stock-assessment information from Maunder and Watters (2002) to develop an empirical model of how egg production by large fishes in split-pool components might be influenced by SST. We obtained a maximum likelihood estimate of the rate parameter for this model by fitting to data on relative recruitment (time-specific recruitments divided by an average recruitment).

$$(5) \qquad r^*_{it} = \exp(-0.131X_t)$$

where $i \in$ {Sm marlins, Sm dorado, Sm yellowfin, Sm sailfish, Sm wahoo, Sm bigeye, Sm swordfish}. We generated series of $r^*_{it}$ by entering NIÑO3 SST anomalies into eq. 5, and we substituted these series of $r^*_{it}$ into eq. 2. Thus, we forced egg production to increase during warm events and decrease during cold events.

## Simulations

We used eqs. 3–5 to construct two scenarios by which physical forces affect the pelagic ecosystem in the ETP. We use the term scenario because eqs. 3–5 are correlative, not mechanistic. For scenario 1, we used only eq. 3 to drive the ecosystem. Scenario 1 modeled only bottom-up forcing of large phytoplankton biomass, and we categorized the effects of this scenario on middle and upper trophic levels as indirect. For scenario 2, we used eqs. 3–5 simultaneously. Scenario 2 modeled the combined effects of forcing large phytoplankton biomass and predator recruitment. We categorized environmental effects on recruitment as direct, and therefore, scenario 2 included both indirect and direct environmental effects on components at middle and upper trophic levels. Comparing the results of simulations forced under scenario 1 with those forced under scenario 2 allowed us to consider interactions between the indirect and direct effects of physical forcing.

**Fig. 2.** Simulated effects, under scenario 1, of single pulses in the biomass of large phytoplankton corresponding to ±2 °C pulses in sea-surface temperature. The trophic level of each component from (*a*) the axis of the *Auxis* and (*b*) the axis of the squid is indicated in parentheses. Lg, large; Sm, small; Misc., miscellaneous.

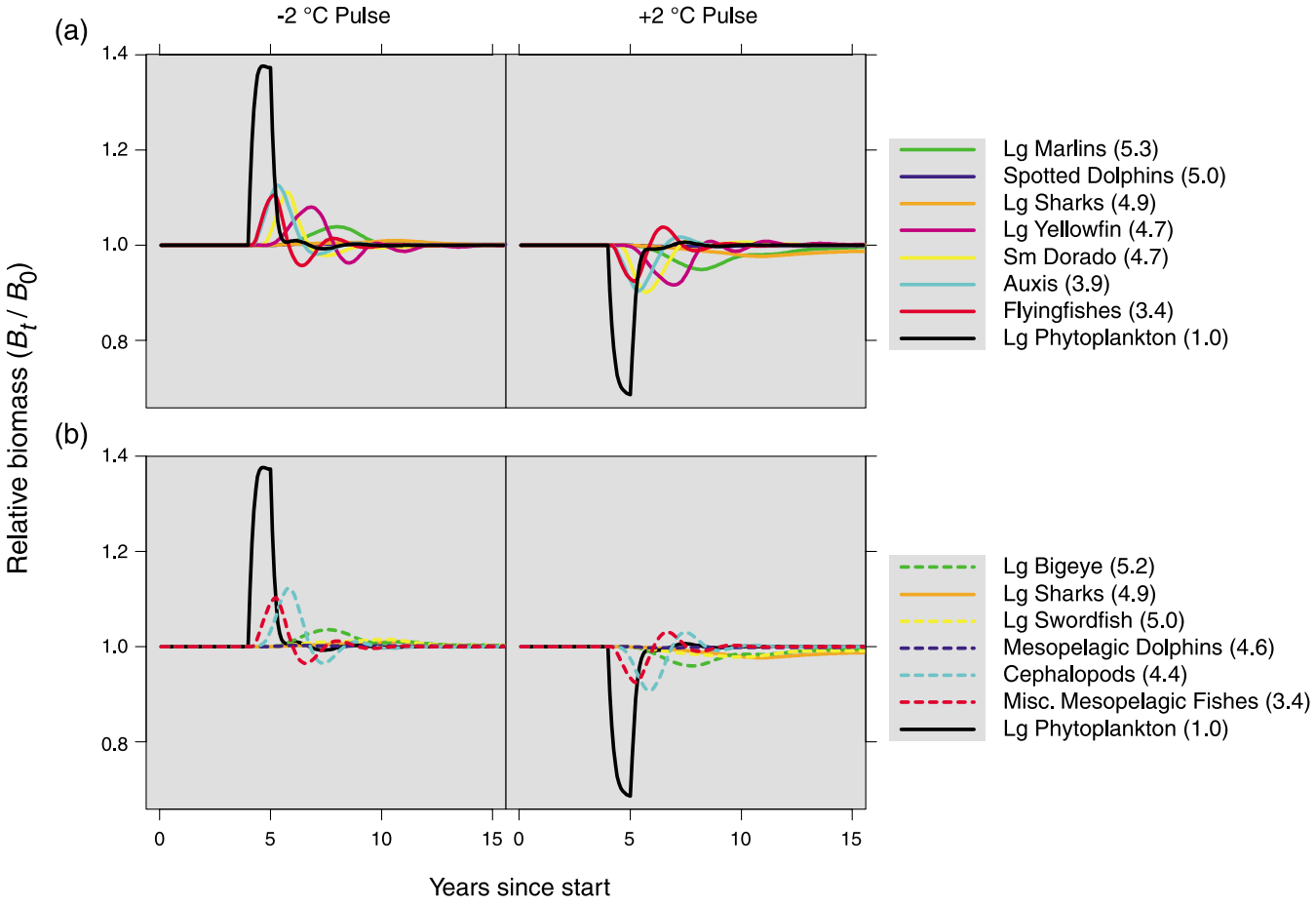


We ran three sets of simulations under each scenario. In the first set, we substituted positive and negative climate-anomaly pulses (±2 °C SST anomalies) for $X_t$ in eqs. 3–5. We chose these anomalies because they span the dynamic range of most anomalies observed in the NIÑO3 time series. Each pulse was specified to occur for 1 year during a 50-year simulation.

In the second set of simulations, we substituted regular climate cycles (corresponding to alternating ±2 °C SST anomalies) for $X_t$ in eqs. 3–5. We considered ENSO-scale cycles with 2-, 4-, and 6-year periods and with "early", "even", and "late" cadences. We defined cadence according to the relative position of a cold event within a single warm–cold cycle. Cycles with even cadence had a cold event occurring exactly halfway between two successive warm events. Early cadence was when the cold event occurred during the first half of a cycle, and late cadence was when the cold event occurred during the second half of a cycle. We structured the second set of simulations so that one cold event always fell between successive warm events.

In the final set of simulations, the ecosystem was driven with NIÑO3 SST anomalies predicted from three models of greenhouse warming. We used means of winter (November–March) anomalies predicted from the Max Planck global climate model (GCM; referred to as the ECHAM4/OPYC3 coupled general circulation model by Timmermann et al. (1999)) and the second and third versions of the Hadley Centre coupled model (HadCM2 from Collins (2000*a*); HadCM3 from Collins et al. (2001)). The ENSO signals in these global-warming scenarios are complex. There are subtle changes in both the frequency and cadence of warm and cold events, and there are successive warm events without intervening cold events (and vice versa). The global-warming scenarios are further characterized by long-term increases in SST. Using eqs. 3–5, we translated these trends into long-term reductions in large phytoplankton biomass and increases in predator recruitment. We used winter SST anomalies in this set of simulations because our work focused on interannual change, and in the ETP, ENSO-induced variations in SST are typically amplified during this season.

Fishing mortality rates ($F$) were specified for each set of simulations. In the first two sets, $F$s were constant and equal to the average $F$ estimated to have affected each component during 1993–1997 (the $F$s that Olson and Watters (2003) used to compute a mass balance). Two levels of $F$ were used in the third set of simulations: $F$ = average $F$ during 1993–1997, and $F = 0$. Components that were subjected to $F$ are listed in Table 1, and uncertainty surrounds the average $F$s that we used.

We summarized our results by focusing on two subsets of components from the ecosystem. We named these subsets "axis of the *Auxis*" and "axis of the squid". The trophic

**Fig. 3.** Spearman rank correlations (rho) between large phytoplankton and all other components of the ecosystem. The model was forced with an historical series (1900–1999) of NIÑO3 sea-surface temperature anomalies. Correlations were computed at lags of 0, 1, and 2 years. (*a*) Results from scenario 1; (*b*) results from scenario 2. The points marked "A" are large phytoplankton – large phytoplankton correlations; the points marked "B" are large phytoplankton – *Auxis* correlations; the points marked "C" are large phytoplankton – small yellowfin correlations; and the points marked "D" are large phytoplankton – large yellowfin correlations. The solid dots are correlations between large phytoplankton and all other components of the ecosystem.

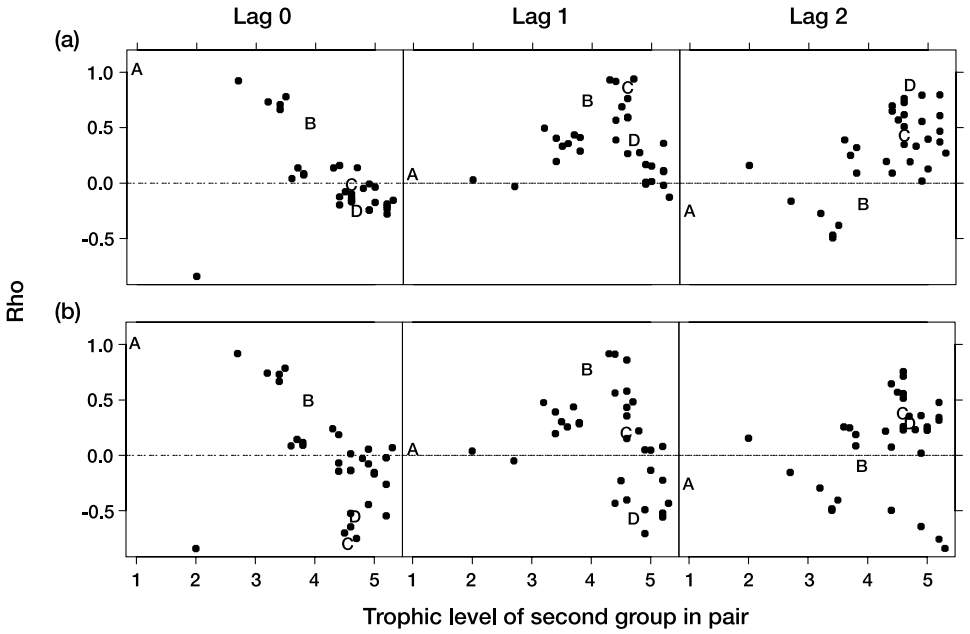


pathways within these subsets are illustrated in Fig. 1. We chose these subsets for four practical reasons. First, each axis includes predators that are of interest from both utilization and conservation perspectives (e.g., large yellowfin and large sharks). Second, the components within each axis have simulated biomass trajectories that bracket the dynamic range of the responses that we predicted (e.g., *Auxis* and cephalopods trajectories were highly variable). Third, the components within each axis illustrate patterns and trends that were representative of groups not included in either axis (e.g., trends for flyingfishes were representative of those for miscellaneous epipelagic fishes). Finally, there are direct trophic linkages, including cannibalism, between the components of each axis (e.g., large bigeye eat cephalopods, and cephalopods are cannibalistic). The axes represent two pathways by which energy derived from bottom-up forcing can flow to the middle and upper trophic levels, but these axes are not alternative system states.

## Results

### ENSO-scale effects from scenario 1

Bottom-up pulses of large phytoplankton biomass, corresponding to ±2 °C SST anomalies, caused the biomasses of most ecosystem components to oscillate (Fig. 2). These oscillations often propagated for years after the pulse. Responses to pulses in large phytoplankton biomass were related to trophic level, but not to whether ecosystem components were members of the axis of the *Auxis* or the axis of the squid. Pulse-induced variations in biomass were greatest for components at middle trophic levels (e.g., flyingfishes, *Auxis*, small dorado, miscellaneous mesopelagic fishes, and cephalopods) and lowest for components at upper trophic levels (e.g., large sharks, large swordfish, and large marlins). In general, responses to bottom-up pulses were lagged, and the lag increased with increasing trophic level. For some components at high trophic levels, the effects of negative bottom-up pulses (positive SST anomalies) were longer in duration than those of positive bottom-up pulses (negative SST anomalies). Marine mammals did not respond to bottom-up pulses, and pulses did not kick the system into alternative states (all biomass trajectories eventually returned to their initial conditions).

We further examined lags in responses to bottom-up forcing with an historical series (1900–1999) of winter mean NIÑO3 SST anomalies computed from data provided by Kaplan et al. (1998) and Reynolds and Smith (1994). We obtained these data from the LDEO/IRI Data Library at http://ingrid.ldeo.columbia.edu. We computed pairwise correlations between large phytoplankton biomass and the biomasses of all other components at lags of 0, 1, and 2 years. Lower trophic levels were correlated with the large phytoplankton at short lags; middle trophic levels were correlated with the large phytoplankton at medium lags; and upper trophic levels were correlated with the large phytoplankton at long lags (Fig. 3). Bottom-up effects acted as trophic waves that propagated through the ecosystem.

Changing the period and cadence of regular cycles in large phytoplankton biomass affected the oscillatory patterns of biomass trajectories for components at middle and upper trophic levels. As the period of bottom-up cycles increased, the period of cycles in other ecosystem components also increased (Fig. 4). Increasing the period of warm–cold cycles also caused the trajectories of some ecosystem components (e.g., flyingfishes and small dorado) to become mixtures of waves with different amplitudes (Fig. 4). As with bottom-up

**Fig. 4.** Simulated effects, under scenario 1, of regular, warm–cold cycles on components in the axis of the *Auxis*. The heading at the top of each panel indicates the structure of the cycle that was used to force the model. "W" indicates warm events (2 °C sea-surface temperature (SST) anomalies), "C" indicates cold events (–2 °C SST anomalies); and dash (–) indicates average conditions (0 °C SST anomalies). Panels in the middle row illustrate simulations with 2-, 4-, and 6-year periods (from left to right); the climate drivers for all of these simulations had even cadences. Panels in the middle column illustrate simulations with "early", "even", and "late" cadences (from top to bottom); all of these simulations had forcing with a 4-year period. The trophic level of each component is indicated in parentheses. Lg, large; Sm, small.

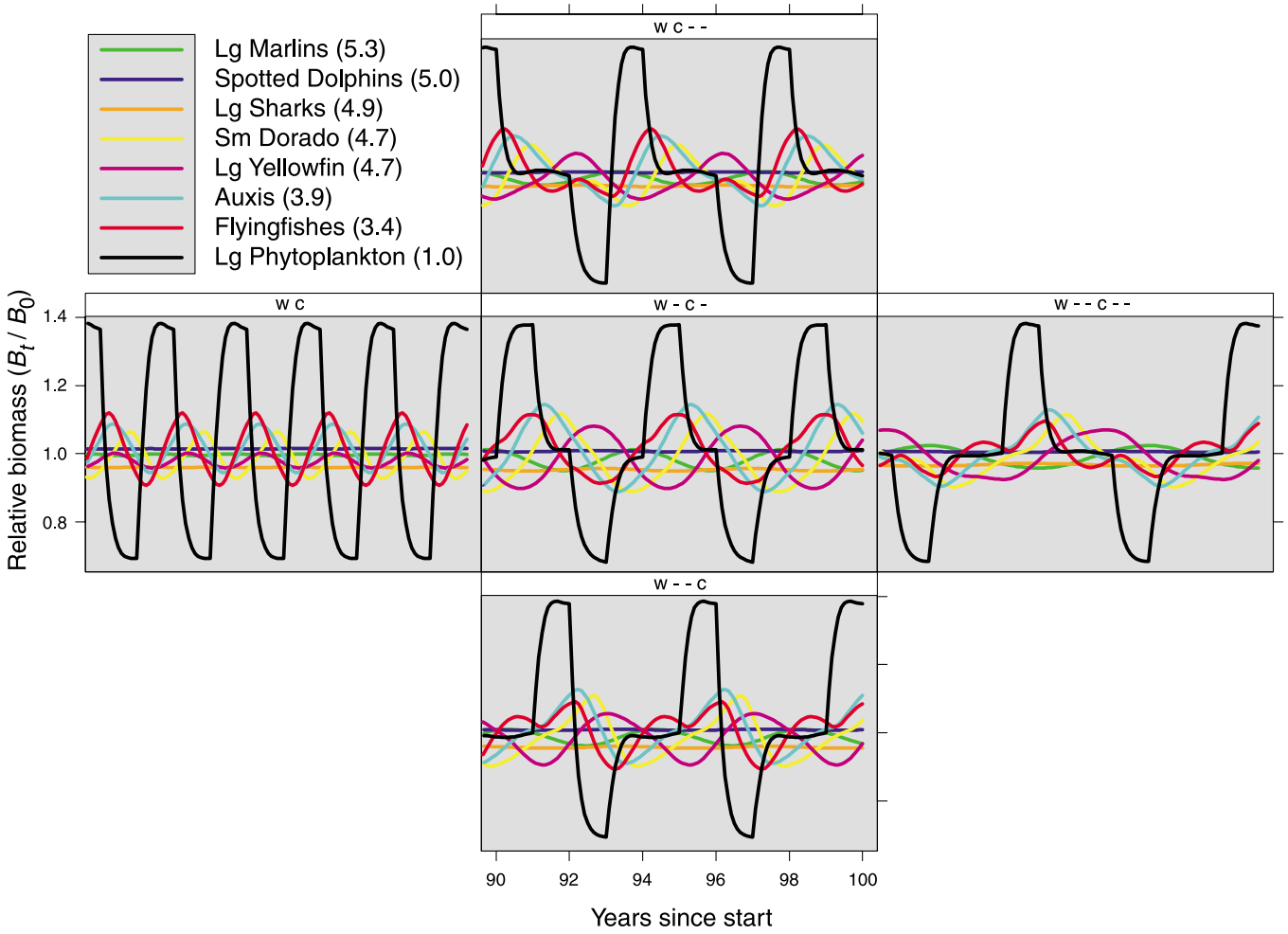


pulses, the amplitudes of these oscillations decreased with increasing trophic level. Changing the period of ENSO-scale cycles in the biomass of large phytoplankton had small, but seemingly biologically insignificant, effects on the means and variances (computed over a single cycle) of the biomass trajectories for other components in the model (results not shown). Changing the cadence of the bottom-up forcing affected animals at middle and upper trophic levels in a manner similar to that of changing the period. Although most biomass trajectories were sensitive to the period and cadence of ENSO forcing, none of the cyclic-forcing simulations predicted that the ecosystem would be restructured by the extinction or explosion of one or more components (Fig. 4).

### ENSO-scale effects from scenario 2

Forcing under scenario 2 changed both the short- and long-term predictions from our ecosystem model. The short-term effect was that the biomasses of all split-pool components (except sharks because they were not forced under scenario 2) increased immediately after a reduction in large phytoplankton biomass (a warm event) (Fig. 5). After this increase, the biomasses of split-pool components declined, and the trajectories fell into phase with the predictions made under scenario 1 (Fig. 5). The long-term effect of forcing under scenario 2 was to increase variability in the biomass trajectories of split-pool components (Fig. 5). When the historical series (1900–1999) of NIÑO3 SST anomalies was used to force the model, the ecosystem was not restructured by split-pool components that either capitalized on a series of warm events or suffered from a series of cold events (Fig. 5). Negative correlations between the biomasses of large phytoplankton and components at upper trophic levels were more common under scenario 2 than scenario 1 (Fig. 3).

### Global-warming effects

We reiterate that the SST anomalies used to drive the set of global-warming simulations contain complex combinations of ENSO periods and cadences superimposed on long-term

**Fig. 5.** Biomass trajectories for large phytoplankton (thick solid lines) and yellowfin tuna predicted under scenarios 1 (thin solid lines) and 2 (thin broken lines). The panels in row (*a*) are for small yellowfin, and the panels in row (*b*) are for large yellowfin. SST, sea-surface temperature.

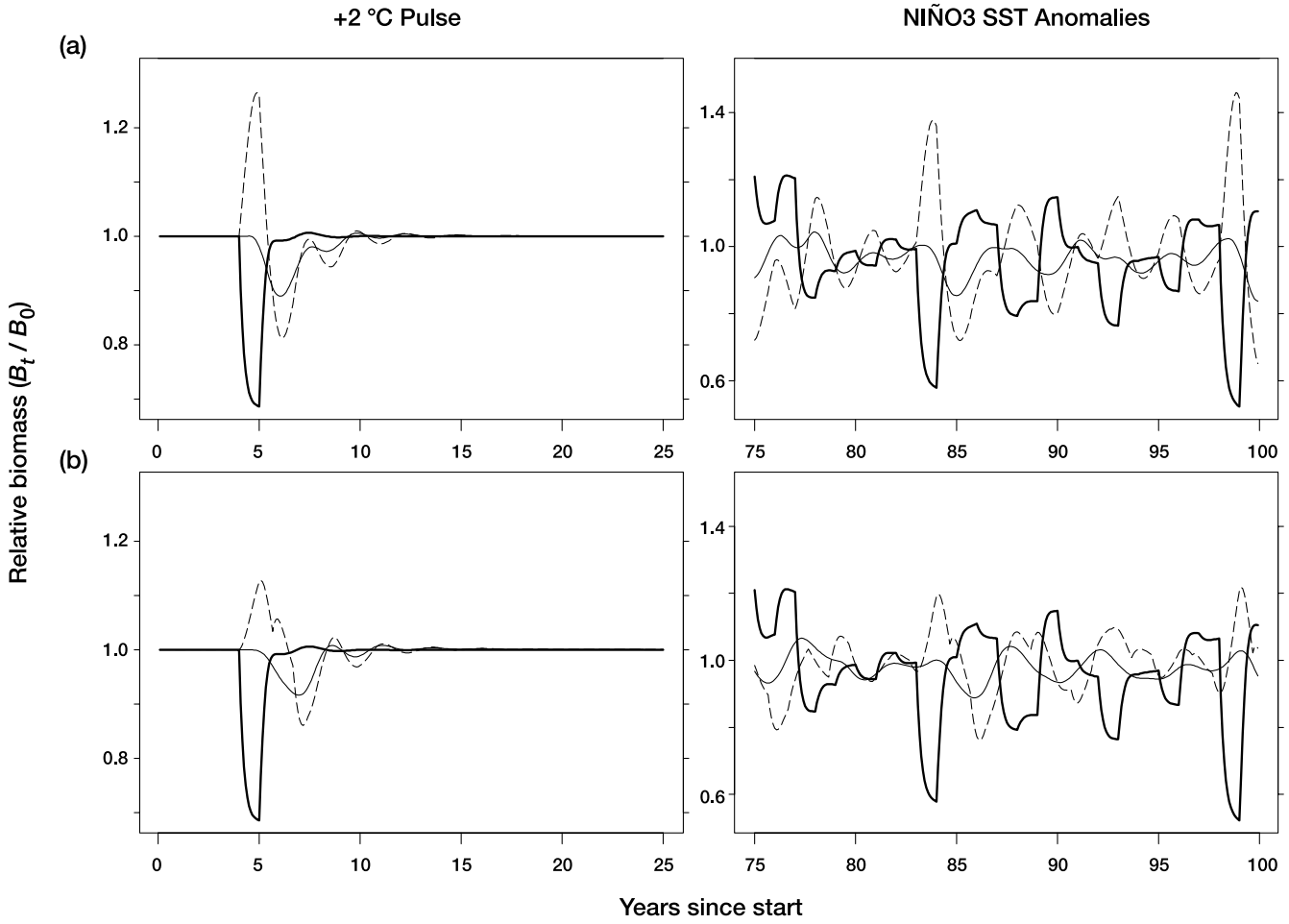


warming trends. To decouple the periodicity and warming effects, we analyzed the simulated biomass trajectories with wavelets (Torrence and Compo 1998). Although the Max Plank GCM, the HadCM2, and the HadCM3 predict different ENSO patterns (and therefore different estimates of biomass at any specific time), our wavelet analyses of the biomass trajectories predicted from these three climate models gave similar results. Therefore, all further references to the global-warming simulations are to the Max Planck GCM.

The time-averaged wavelet spectra of many biomass trajectories predicted from our global-warming simulations were characterized by significantly high power at periods of about 1.5–6 years (Table 3). The components with spectra displaying this feature were sensitive to ENSO-scale forcing during global warming. Significantly high power at short periods was typical of spectra from components with relatively high *Z*s (Table 3). These results were robust to the differences between scenarios 1 and 2, but forcing under scenario 2 caused some components with relatively low *Z*s (e.g., large marlins and large bigeye) to be sensitive to ENSO-scale forcing (Table 3). Components with *Z*s less than about 0.5 were not sensitive to ENSO-scale forcing during global warming (Table 3).

The time-averaged wavelet spectra of all biomass trajectories from the global-warming simulations were also characterized by a steady increase in power with increasing period (Table 3). This result was obtained under both forcing scenarios, and it illustrated the importance of the global-warming trend. Under scenario 1, long-term warming was predicted to reduce the relative biomasses of all ecosystem components (Fig. 6). These reductions were predicted regardless of whether the simulation included fishing mortality, but the absence of fishing mitigated the impact of warming on some predators (e.g., large sharks, large marlins, and large yellowfin) (Fig. 6). Under scenario 2, long-term warming was predicted to increase the relative biomasses of all split-pool components except sharks (Fig. 7). These components benefited from an increasing trend in recruitment.

We also used variance-components models to analyze the biomass trajectories predicted from the global-warming simulations. We treated the two levels of *F* used in these simulations (*F* = average *F* during 1993–1997, and *F* = 0) as random effects and estimated the fraction of the total variation in the two trajectories predicted for each component that was explained by differences in *F*. These variance ratios were estimated by maximum likelihood and ranged from 0

**Table 3.** Characteristics of the time-averaged power spectra of various biomass trajectories predicted by forcing the ecosystem model with 21st century sea-surface temperature anomalies from the Max Planck global climate model.

| | Significantly high power at periods of about 1.5– 6 years | | Power increases as the period increases | |
|---|---|---|---|---|
| Component (*Z*) | Scenario 1 | Scenario 2 | Scenario 1 | Scenario 2 |
| **Axis of the *Auxis*** | | | | |
| Spotted dolphins (0.04) | | | × | × |
| Lg sharks[a] (0.32) | | | × | × |
| Lg marlins (1.00) | | × | × | × |
| Lg yellowfin (2.35) | × | × | × | × |
| *Auxis* (2.50) | × | × | × | × |
| Flyingfishes (2.88) | × | × | × | × |
| Sm dorado (3.15) | × | × | × | × |
| Lg phytoplankton[a] (125.00) | × | × | × | × |
| **Axis of the squid** | | | | |
| Mesopelagic dolphins (0.04) | | | × | × |
| Lg swordfish (0.44) | | | × | × |
| Lg bigeye (0.76) | | × | × | × |
| Cephalopods (2.00) | × | × | × | × |
| Misc. mesopelagic fishes (2.00) | × | × | × | × |

**Note:** A red-noise spectrum (AR(1)) was used to determine significance at $\alpha = 0.10$. The ecosystem components are sorted by *Z*. Lg, large; Sm, small; Misc., miscellaneous.

[a]These components are members of both axes.

(for large phytoplankton) to levels greater than 0.9 (for predators like large sharks, large swordfish, large yellowfin, and large bigeye) (Table 4). We used the variance ratios to measure the degree to which fishing and physical forcing shaped the dynamics of each ecosystem component. We interpreted relatively low variance ratios as indicators of control by physical forces and relatively high ratios as indicators of control by fishing. Intermediate variance ratios were considered to be indicative of mixed control.

The degree to which each component of the ecosystem appeared to be controlled by fishing or physics was related to the ratio $F/Z$ (where $F$ = average $F$ during 1993–1997, and $Z$s are from Table 1). In general, components that were subjected to little or no fishing mortality (e.g., flyingfishes, cephalopods, and miscellaneous mesopelagic fishes) were controlled by physical forces. Marine mammals were, however, an exception to the latter result, and mammals appeared to be controlled by a mix of physical forces and fishing. Fishery targets and dominant bycatch species (e.g., large yellowfin, large bigeye, large sharks, and large marlins) were controlled by fishing rather than physics (Table 4). These results were generally robust to the differences between scenarios 1 and 2, but the variance ratios predicted from forcing under scenario 2 were almost always less than those predicted by forcing under scenario 1 (Table 4).

## Discussion

We do not claim that our ecosystem model can accurately predict future levels of biomass; too much uncertainty surrounds our parameter estimates. Nevertheless, Olson and Watters (2003) provide results indicating that the ETP model may be a useful tool for studying how physical variability influences food-web dynamics. From an initial sensitivity analysis, Olson and Watters (2003) determined that the mass-balance allocation of energy among model components was most sensitive to parameter values for the cephalopods and *Auxis*. Because there is also substantial uncertainty surrounding the parameters for cephalopods and *Auxis*, Olson and Watters conducted a second sensitivity analysis to consider whether changing the parameters for these two components would affect (1) time-series predictions from Ecosim and (2) the model's fit to time-series data on yellowfin and bigeye tunas. In the former case, Olson and Watters found that changing parameter values for cephalopods and *Auxis* affected the scaling of biomasses predicted by Ecosim but had negligible effects on the prediction of trends. In the latter case, Olson and Watters found that goodness of fit to the data on yellowfin and bigeye tunas was usually degraded by changing the parameters for cephalopods and *Auxis* (sums of squares were increased from 0.2 to 69.7%). In a few cases, the goodness of fit was increased, but the largest such increase represented only a 3.3% reduction in the sum of squares. In our opinion, the results of Olson and Watters (2003) suggest that our focus on variability in future biomass, rather than actual levels of biomass, is appropriate.

### Indirect effects from ENSO-scale variability in plant biomass

Results from both the pulse-forcing and cyclic-forcing simulations suggested that the biomass trajectories of components at upper trophic levels are less sensitive to ENSO-scale changes in large phytoplankton biomass than those of components at middle trophic levels. To some degree, this result is trivial because energy is lost during transfer between trophic levels, but life-history differences also shape responses to bottom-up forcing. In the ETP, predators like sharks and marlins consume animals from a wide range of trophic lev-

**Fig. 6.** The simulated effects, under scenario 1, of global warming on components in the axis of the *Auxis* ((*a*) large marlins, (*b*) spotted dolphins, (*c*) large sharks, (*d*) small dorado, (*e*) large yellowfin, (*f*) *Auxis*, (*g*) flyingfishes, and (*h*) large phytoplankton). The simulations were forced with winter mean sea-surface temperature anomalies predicted by the Max Planck global climate model. Solid lines are from simulations with $F$ = average $F$ during 1993–1997, and broken lines are from simulations with $F$ = 0. A horizontal broken line is drawn for reference at $B_t/B_0$ = 1.0.

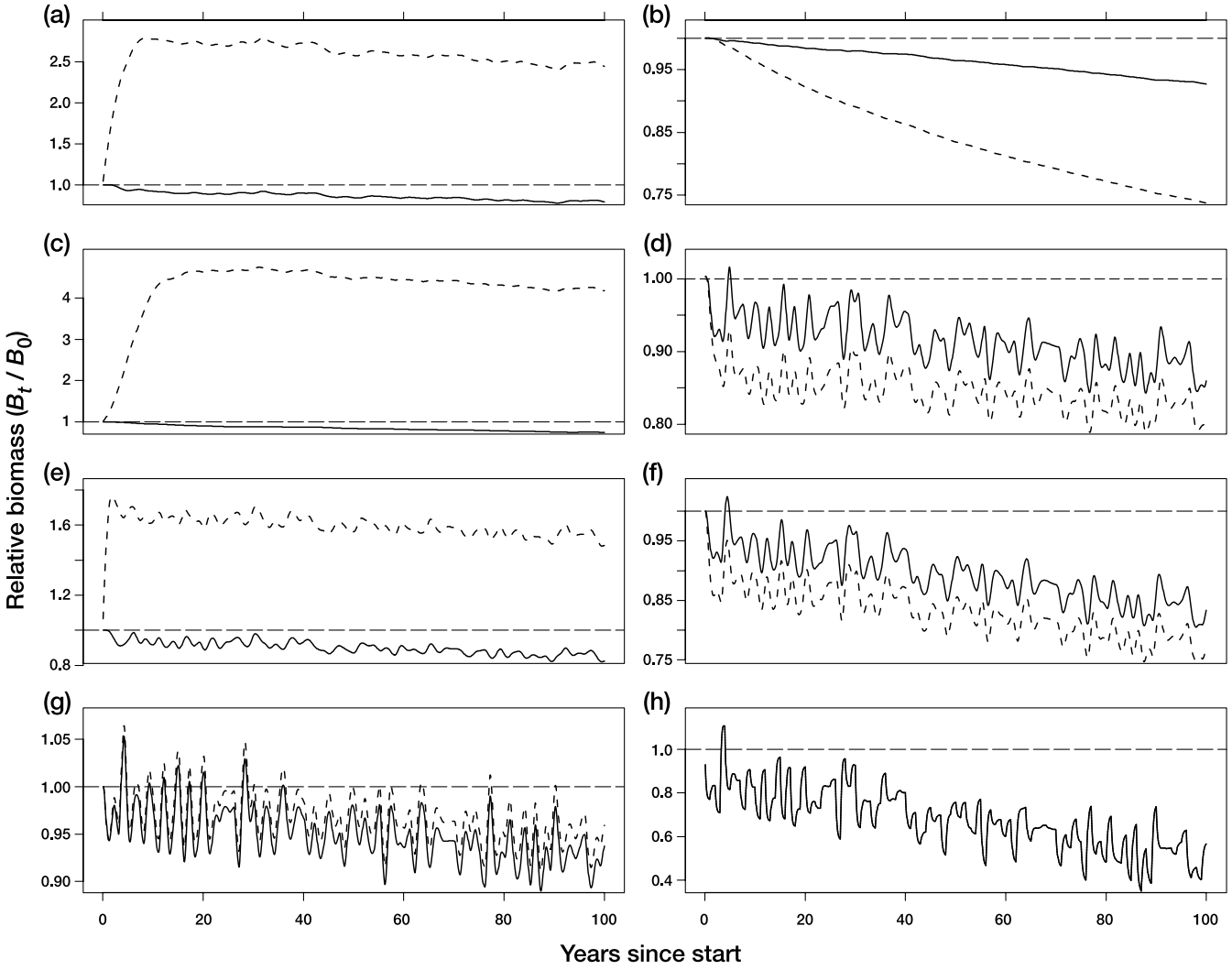


els (Olson and Watters 2003). These predators smooth through bottom-up variability by utilizing energy from different regions of the trophic pyramid. Some predators in the ETP, like dolphins, are also relatively unproductive, and despite having varied diets, their populations cannot respond quickly to short-term increases in bottom-up productivity. In contrast, components at middle trophic levels, like flyingfishes and cephalopods, prey on animals from a more narrow range of trophic levels and are highly productive. Less varied diets and high rates of productivity make components at middle trophic levels more sensitive to short-term changes in phytoplankton biomass.

Results from the pulse-forcing and cyclic-forcing simulations also showed how the bottom-up effects of individual climate events (e.g., El Niños and La Niñas) can be complicated by ecological interactions. Under scenario 1, biomass trajectories often trended in the opposite direction of the physical forcing because of combinations of interspecific (top-down) and intraspecific (density-dependent) effects. For example, a reduction in the biomass of flyingfishes was predicted to occur about 1 year after an increase in large phytoplankton biomass. Interspecific and intraspecific effects also caused many of the biomass trajectories predicted from the cyclic-forcing simulations to behave like complex mixtures of waves, despite the fact that our cyclic-forcing functions were simple.

It seems unlikely that one could monitor an individual population or stock (perhaps with stock assessments or research surveys) and determine whether individual peaks and valleys in a time series of biomass estimates resulted from bottom-up forcing. It takes time for variations in plant biomass to cascade through the system, and the lag of the response time is a function of each component's trophic level. To detect the indirect effects of climate on middle and upper trophic levels, one will need to monitor a suite of populations or stocks that are connected through predator–prey in-

**Fig. 7.** The simulated effects, under scenario 2, of global warming on components in the axis of the *Auxis* ((*a*) large Marlins, (*b*) spotted dolphins, (*c*) large sharks, (*d*) small dorado, (*e*) large yellowfin, (*f*) *Auxis*, (*g*) flyingfishes, and (*h*) large phytoplankton). The simulations were forced with winter mean sea-surface temperature anomalies predicted by the Max Planck global climate model. Solid lines are from simulations with $F$ = average $F$ during 1993–1997, and broken lines are from simulations with $F$ = 0. A horizontal broken line is drawn for reference at $B_t/B_0$ = 1.0.

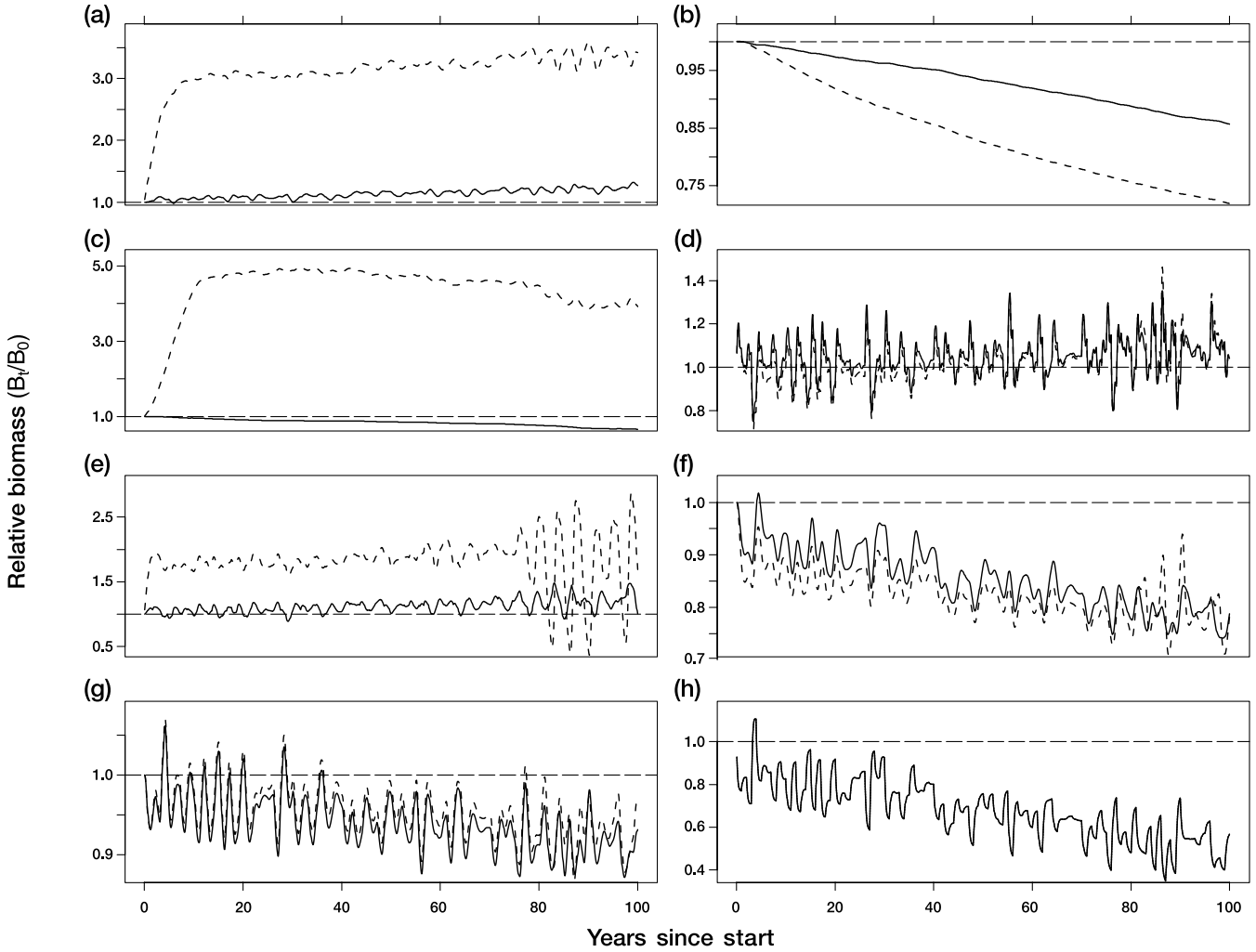


teractions. Bottom-up signals can only be detected by their propagation through the food web.

**Direct ENSO-scale effects**

Comparing our results with those from the meta-analysis conducted by Micheli (1999) provides a useful background for discussing the importance of the direct effects of climate on middle and upper trophic levels. Although Micheli found a positive correlation between primary productivity and phytoplankton biomass, positive correlations between primary productivity and the biomasses of both mesozooplankton and zooplanktivorous fishes were found in only two of 20 pelagic marine systems. Micheli (1999) concluded that changes in primary productivity "rarely cascade upward to affect biomass of marine pelagic consumers". Our predictions from scenario 1, when considered jointly with previous observations of coupling between primary production and phytoplankton biomass in the ETP (e.g., Barber et al. 1996), were not consistent with this conclusion. In fact, scenario 1 predicted positive correlations between large phytoplankton biomass and the biomasses of most other components in the system, particularly if time lags were considered. Although it is not apparent that Micheli's meta-analysis considered time lags, we suggest that the absence of direct physical effects in scenario 1 is responsible for the apparent contradiction.

Micheli (1999) proposed three possible mechanisms to explain weak coupling between phytoplankton and herbivores; we offer a fourth possibility provoked by our predictions from scenario 2. We noticed that scenarios 1 and 2 predicted nearly identical correlations between large phytoplankton and components with trophic levels less than about 4.0. In contrast, the two mechanisms predicted less similar correlations between large phytoplankton and components with trophic levels greater than 4.0. Under scenario 1, all climate effects on upper trophic levels were indirect, but under scenario 2, 14 of the 25 components with trophic levels greater than 4.0 were also forced by direct effects on recruitment. We conclude that the relative strengths of indirect and direct physical effects can determine both the sign and scale of correlations between consumer groups and producer groups. Thus, a fourth way to explain Micheli's (1999) finding of

**Table 4.** Variance ratios from the global-warming simulations.

| Component (*F*/*Z*) | Scenario 1 | Scenario 2 |
|---|---|---|
| **Axis of the *Auxis*** | | |
| Lg marlins (0.50) | 0.97 | 0.95 |
| Lg sharks[a] (0.48) | 0.93 | 0.92 |
| Lg yellowfin (0.35) | 0.98 | 0.64 |
| Spotted dolphins (0.03) | 0.53 | 0.35 |
| Sm dorado (0.01) | 0.53 | 0.01 |
| *Auxis* (0.00) | 0.34 | 0.07 |
| Flyingfishes (0.00) | 0.10 | 0.04 |
| Lg phytoplankton[a] (0.00) | 0.00 | 0.00 |
| **Axis of the squid** | | |
| Lg swordfish (0.75) | 0.92 | 0.91 |
| Lg bigeye (0.31) | 0.97 | 0.93 |
| Mesopelagic dolphins (0.00) | 0.55 | 0.44 |
| Cephalopods (0.00) | 0.02 | 0.00 |
| Misc. Mesopelagic Fishes (0.00) | 0.00 | 0.00 |

**Note:** Each ratio is the fraction of the total variation in two biomass trajectories (see Figs. 6 and 7) explained by the differences in fishing mortality ($F$ = average $F$ during 1993–1997, and $F = 0$). The ecosystem components are sorted by $F/Z$. Lg, large; Sm, small; Misc., miscellaneous.
[a]These components are members of both axes.

weak coupling between phytoplankton and herbivores is that herbivore populations are often subjected to direct physical effects on reproduction and growth, and these direct effects frequently dampen signals generated from bottom-up forcing. Our model does not currently include direct effects on consumers at low and middle trophic levels, but the literature contains references that recognize such effects in other systems influenced by the ENSO (e.g., Barber and Chávez 1986).

Our work suggests that under constant fishing mortality, direct physical effects are the dominant sources of interannual variation in the biomasses of consumer groups from the ETP. This statement hinges on our inclination to consider scenario 2 more realistic than scenario 1. We provide two reasons for this preference. First, given the discussion in the previous two paragraphs, scenario 1 seems less reasonable. Second, scenario 2 predicted a level of variation in small yellowfin biomass that was closer to the amount of variation in annual recruitment estimated for yellowfin tuna. The coefficient of variation (CV) in estimates of annual recruitment for yellowfin tuna is about 0.25 (Maunder and Watters 2002), and using winter mean NIÑO3 SST anomalies, CVs predicted from scenarios 1 and 2 were about 0.04 and 0.12, respectively.

It seems reasonable to ask how it is possible for predator recruitment to increase after an El Niño (e.g., Maunder and Watters 2002) despite observations of reduced phytoplankton biomass during these events (e.g., Barber et al. 1996). Presumably, even if large predators produce more eggs and small predators are themselves less vulnerable to predation, the recruits would still have to be supported by production from the bottom of the food web. In the ETP, it appears as if this support comes from the picoplankton. We did not model ENSO-driven changes in the biomass of small producers because measurements from flow cytometry (Landry et al. 1996) and estimates of the size fractionation of phytoplankton pigments (Bidigare and Ondrusek 1996) support the conclusion that there is less temporal variation in picoplankton biomass than in the biomasses of large cells like diatoms. These studies also show that picoplankton account for most of the plant biomass and production in the equatorial Pacific Ocean. The relatively large and temporally conservative biomass of picoplankton further supports our view that, given a constant level of fishing mortality, most of the interannual variations in the biomasses of consumer groups from the ETP are propagated by the direct, rather than indirect, effects of climate.

## Global-warming effects

Regardless of how global warming affects the pattern of the ENSO, all components of the pelagic ecosystem in the ETP may be sensitive to long-term changes in the physical environment. Fishing may both mitigate and reinforce the effects of global warming. Sustained reductions in fishing mortality might mitigate the effects of global warming on components that are currently experiencing high levels of $F$ relative to $Z$ (e.g., large marlins, large sharks, and large yellowfin). The biomasses of other components (e.g., small dorado and *Auxis*) might be reduced by decreased levels of $F$ because predation mortality on these components would be increased. Substantial reductions in $F$ might also reduce the biomasses of components that feed on the same prey as the large fishes (e.g., spotted dolphins). Our results are consistent with a conclusion that has been made by other workers (e.g., Jurado-Molina and Livingston 2002): the effects of future climate change need to be considered in combination with future levels of fishing mortality.

Responses to global warming will also be affected by the degrees to which indirect and direct effects play a role in forcing the system. Direct, positive effects of global warming on predator recruitment can potentially compensate for a reduction in total plant biomass if some phytoplankton are not adversely affected by such climate change. In the ETP, the large and temporally stable biomass of picoplankton may provide the necessary base for consumers to profit from global warming. We note, however, that biogeochemical cycling and its effect on the bottom of the food web in the tropical Pacific Ocean is an area of active research, and future workers may find that picoplankton populations can be adversely affected by global warming.

## The top-down effects of fishing

Although either bottom-up (e.g., Roemmich and McGowan 1995) or top-down (e.g., Shiomoto et al. 1997) processes may be the dominant mechanisms structuring marine ecosystems, it seems more robust to acknowledge that these processes act concomitantly (e.g., Verheye and Richardson 1998). In essence, bottom-up forces define a template on which top-down effects may act (Hunter and Price 1992; Power 1992). The effects of fishing are also constrained by this template, and we initiated this study because detecting the ecosystem consequences of fishing in the ETP will eventually require a description of the background variability in this system. Without such a description, we suspect that it will often be difficult to support hypotheses of fishing effects over hypotheses of environmental effects (and vice versa).

It seems likely that the fisheries operating in the ETP are able to control the biomasses of both target species (e.g., bigeye tuna) and bycatch species (e.g., sharks), even if physical variability is considered. Under recent levels of $F$, how-

ever, some bycatch species (e.g., small dorado) are more likely to be controlled by physical forces. The degree to which fisheries control components of the ecosystem is partly determined by levels of *F*, but results from our variance-components analysis suggest that the top-down effects of fishing are less able to cascade through the food web if direct effects are the dominant source of physical variability in the system. This may be our most important conclusion.

**Caveats and conclusions**

Our results were sensitive to the rate parameters in eqs. 3–5, and such simple descriptions of physical–biological linkages may fail after additional data collection and analysis. Failures may occur because models like eqs. 3–5 are not mechanistic and may therefore oversimplify complex processes or describe spurious correlations. Nevertheless, the literature contains evidence supporting hypotheses that both phytoplankton biomass (see Introduction) and predator recruitment (see Methods) are affected by climate. Our estimates of the rate parameters determined both the scales of our predictions and the relative differences among the predictions from scenarios 1 and 2. We also assumed that the rate parameters in eqs. 3–5 are stationary. It seems reasonable to hypothesize that these rates would change over time, and further simulations with nonstationary rate parameters would be interesting.

Our use of EwE may have affected our conclusions. Projecting forward from a mass-balance "snapshot" may be misleading if the system was never actually in balance. Nevertheless, we found the approach amenable given that the data, particularly the diet compositions, used to parameterize the model were themselves snapshots. Two other aspects are perhaps more troublesome. First, models like ours that aggregate over large spatial scales, many species, and multiple age structures are likely to be less responsive to the effects of fishing than models with less aggregation (Cox et al. 2002). Responsiveness to environmental effects is also likely to be influenced by the level of aggregation in a model (Rice 1995), and it would be interesting to compare our results with those from models with different numbers of components. Second, although we investigated model uncertainty by considering two forcing scenarios, the predator–prey dynamics in EwE are limited to the family of behaviors that can be described by eq. 3. Rice (2001) notes that the effects of physical forcing need to be investigated in the context of consumer groups that participate in scramble competition (all consumers undergoing simultaneous periods of food shortage or excess). This appears to be particularly relevant to regime shifts. Regime shifts may occur in the ETP (McPhaden and Zhang 2002; Chavez et al. 2003), but we did not simulate this type of forcing. We acknowledge, therefore, that there are likely to be dynamic behaviors, both ecological and physical, that dampen or intensify the patterns described here.

Our global-warming simulations predicted considerable hypothetical changes in the upper trophic levels of the ecosystem, but these changes may not occur if populations can redistribute spatially. Most of the animals at upper trophic levels are mobile, and large-scale spatial displacements seem likely. For example, the distribution of skipjack tuna in the western Pacific Ocean is linked to large, zonal displacements of the equatorial warm pool (e.g., Lehodey et al. 1997). Range displacement may further complicate predictions about the effects of global warming because large-scale climate changes can also be expected at temperate latitudes (Meehl et al. 1993; Collins 2000*b*). Finally, despite the possibility of range shifts, genetic adaptation or physiological compensation to climate change may occur (Fields et al. 1993; Wood and McDonald 1997).

Our model focused on the ETP, but the following conclusions might be general. First, it will be difficult to detect bottom-up signals in biomass trajectories of single populations, and therefore, workers should look for such signals propagating through a set of biomass trajectories linked by predator–prey interactions. Second, physical forcing that acts directly on animals at middle and upper trophic levels (e.g., by affecting recruitment) can be the dominant source of interannual variability (given a constant level of *F*) in the biomasses of pelagic consumers. Following this, it seems likely that the top-down effects of fishing are less able to cascade through food webs that are dominated by direct physical effects. Finally, predictions about the effects of long-term climate change (e.g., global warming) on animals at middle and upper trophic levels may be misleading if future levels of *F* are not considered. In developing ecosystem models, it is critical to understand where physical forces interact with food webs (Rice 2001). Our results clearly illustrate that predictions from these models are sensitive to the relative strengths of indirect and direct physical effects on middle and upper trophic levels.

## Acknowledgements

This work was conducted by the Ecological Implications of Alternative Fishing Strategies for Apex Predators Working Group. The Working Group was jointly supported by the National Center for Ecological Analysis and Synthesis (NCEAS; Grant No. DEB-94-21535) and the Inter-American Tropical Tuna Commission. The NCEAS is funded by the United States National Science Foundation, the University of California at Santa Barbara, and the State of California. We thank the NCEAS staff for their assistance. We are grateful to Matthew Collins and Axel Timmermann for providing the global-warming forecasts. The manuscript was improved by reviews from William Bayliff, Richard Deriso, Steven Bograd, Franklin Schwing, Steven Martell, and two anonymous referees.

## References

Barber, R.T., and Chavez, F.P. 1983. Biological consequences of El Niño. Science (Wash., D.C.), **222**: 1203–1210.

Barber, R.T., and Chávez, F.P. 1986. Ocean variability in relation to living resources during the 1982–83 El Niño. Nature (Lond.), **319**: 279–285.

Barber, R.T., Sanderson, M.P., Lindley, S.T., Chai, F., Newton, J., Trees, C.C., Foley, D.G., and Chavez, F.P. 1996. Primary productivity and its regulation in the equatorial Pacific during and following the 1991–1992 El Niño. Deep-Sea Res. II Top. Stud. Oceanogr. **43**: 933–969.

Bidigare, R.R., and Ondrusek, M.E. 1996. Spatial and temporal variability of phytoplankton pigment distributions in the central equatorial Pacific Ocean. Deep-Sea Res. II Top. Stud. Oceanogr. **43**: 809–833.

Chavez, F.P., Ryan, J., Lluch-Cota, S.E., and Ñiquen-C., M. 2003. From anchovies to sardines and back: multidecadal change in the Pacific Ocean. Science (Wash., D.C.), **299**: 217–221.

Collins, M. 2000*a*. The El-Niño Southern Oscillation in the second Hadley Centre coupled model and its response to greenhouse warming. J. Climate, **13**: 1299–1312.

Collins, M. 2000*b*. Understanding uncertainties in the response of ENSO to greenhouse warming. Geophys. Res. Letts. **27**: 3509–3513.

Collins, M., Tett, S.F.B., and Cooper, C. 2001. The internal climate variability of HadCM3, a version of the Hadley Centre coupled model without flux adjustments. Clim. Dyn. **17**: 61–81.

Cox, S.P., Essington, T.E., Kitchell, J.F., Martell, S.J.D., Walters, C.J., Boggs, C., and Kaplan, I. 2002. Reconstructing ecosystem dynamics in the central Pacific Ocean, 1952–1998. II. A preliminary assessment of the trophic impacts of fishing and effects on tuna dynamics. Can. J. Fish. Aquat. Sci. **59**: 1736–1747.

Fiedler, P.C., Chavez, F.P., Behringer, D.W., and Reilly, S.B. 1992. Physical and biological effects of Los Niños in the eastern tropical Pacific, 1986–1989. Deep-Sea Res. **39**: 199–219.

Fields, P.A., Graham, J.B., Rosenblatt, R.H., and Somero, G.N. 1993. Effects of expected global climate change on marine faunas. Trends Ecol. Evol. **8**: 361–367.

Hunter, M.D., and Price, P.W. 1992. Playing chutes and ladders: heterogeneity and the relative roles of bottom-up and top-down forces in natural communities. Ecology, **73**: 724–732.

Jurado-Molina, J., and Livingston, P. 2002. Climate-forcing effects on trophically linked groundfish populations: implications for fisheries management. Can. J. Fish. Aquat. Sci. **59**: 1941–1951.

Kaplan, A., Cane, M., Kushnir, Y., Clement, A., Blumenthal, M., and Rajogopalan, B. 1998. Analyses of global sea surface temperature 1856–1991. J. Geophys. Res. **103**: 18 567 – 18 589.

Landry, M.R., Constantinou, J., and Kirshtein, J. 1996. Abundances and distributions of picoplankton populations in the central equatorial Pacific from 12°N to 12°S, 140°W. Deep-Sea Res. II Top. Stud. Oceanogr. **43**: 871–890.

Lehodey, P., Bertignac, M., Hampton, J., Lewis, A., and Picuat, J. 1997. El Niño Southern Oscillation and tuna in the western Pacific. Nature (Lond.), **389**: 715–718.

Maunder, M.N., and Watters, G.M. 2002. Status of yellowfin tuna in the eastern Pacific Ocean. Inter-American Tropical Tuna Commission Stock Assess. Rep. No. 2. pp. 5–90.

McPhaden, M.J., and Zhang, D. 2002. Slowdown of the meridional overturning circulation in the upper Pacific Ocean. Nature (Lond.), **415**: 603–608.

Meehl, G.A., Branstator, G.W., and Washington, W.M. 1993. Tropical Pacific interannual variability and $CO_2$ climate change. J. Climate, **6**: 42–63.

Micheli, F. 1999. Eutrophication, fisheries, and comsumer-resource dynamics in marine pelagic ecosystems. Science (Wash., D.C.), **285**: 1396–1398.

Olson, R.J., and Boggs, C.H. 1986. Apex predation by yellowfin tuna (*Thunnus albacares*): independent estimates from gastric evacuation and stomach contents, bioenergetics, and cesium concentrations. Can. J. Fish. Aquat. Sci. **43**: 1760–1775.

Olson, R.J., and Watters, G.M. 2003. A model of the pelagic ecosystem in the eastern tropical Pacific Ocean. Inter-Am. Trop. Tuna Comm. Bull. **22**: 133–218.

Power, M.E. 1992. Top-down and bottom-up forces in food webs: do plants have primacy? Ecology, **73**: 733–746.

Reynolds, R.W., and Smith, T.M. 1994. Improved global sea surface temperature analysis using optimum interpolation. J. Climate, **7**: 929–948.

Rice, J. 1995. Food web theory, marine food webs, and what climate change may do to northern marine fish populations. *In* Climate change and northern fish populations. *Edited by* R.J. Beamish. Can. Spec. Publ. Fish. Aquat. Sci. No. 121. pp. 561–568.

Rice, J. 2001. Implications of variability on many time scales for scientific advice on sustainable management of living marine resources. Prog. Oceanogr. **49**: 189–209.

Robertson, K.M., and Chivers, S.J. 1997. Prey occurrence in pantropical spotted dolphins, *Stenella attenuata*, from the eastern tropical Pacific. Fish. Bull. U.S. **95**: 334–348.

Roemmich, D., and McGowan, J. 1995. Climatic warming and the decline of zooplankton in the California current. Science (Wash., D.C.), **267**: 1324–1326.

Schaefer, K.M. 1998. Reproductive biology of yellowfin tuna (*Thunnus albacares*) in the eastern Pacific Ocean. Inter-Am. Trop. Tuna Comm. Bull. **21**: 204–272.

Schaefer, K.M. 2001. Assessment of skipjack tuna (*Katsuwonus pelamis*) spawning activity in the eastern Pacific Ocean. Fish. Bull. U.S. **99**: 343–350.

Shiomoto, A., Tadokoro, K., Nagasawa, K., and Ishida, Y. 1997. Trophic relations in the subarctic North Pacific ecosystem: possible feeding effect from pink salmon. Mar. Ecol. Prog. Ser. **150**: 75–85.

Timmermann, A., Oberhuber, J., Bacher, A., Esch, M., Latif, M., and Roeckner, E. 1999. Increased El Niño frequency in a climate model forced by future greenhouse warming. Nature (Lond.), **398**: 694–697.

Torrence, C., and Compo, G.P. 1998. A practical guide to wavelet analysis. Bull. Am. Met. Soc. **79**: 61–78.

Tran, A.V., Smith, E., Hyon, J., Evans, R., Brown, O., and Feldman, G. 1993. Satellite-derived sea surface temperature and phytoplankton pigment concentration data: a CD-ROM set containing monthly mean distributions for the global oceans. Jet Propulsion Laboratory, California Institute of Technology, 4800 Oak Grove Drive, Pasadena, CA 91109.

Verheye, H.M., and Richardson, A.J. 1998. Long-term increase in crustacean zooplankton abundance in the southern Benguela upwelling region (1951–1996): bottom-up or top-down control? ICES J. Mar. Sci. **55**: 803–807.

Walters, C., Pauly, D., Christensen, V., and Kitchell, J.F. 2000. Representing density-dependent consequences of life history strategies in aquatic ecosystems: EcoSim II. Ecosystems, **3**: 70–83.

Wood, C.M., and McDonald, D.G. 1997. Global warming: implications for freshwater and marine fish. Cambridge University Press, Cambridge, U.K.